1 Supplementary Information

1.1 Line-by-line Radiative Transfer Model

To quantify the RF of dust, we performed the radiative transfer calculations using the line-by-line modeling framework. The framework was previously used in (Mok et al., 2016; Osipov et al., 2020) and is described in detail in Appendix A (Osipov et al., 2020). The Python wrapper to run the DISORT model is publicly available at `https://github.com/SeregaOsipov/pyDISORT`. This section outlines the modeling setup adjustments necessary to calculate the RF of aerosols.

We assumed the bright desert Lambertian surface and prescribed an albedo of 0.3. We do not consider the diurnal cycle (see Figure 12 in (Osipov et al., 2015)) and fixed the solar zenith angle at 0 degrees. The dust was distributed in the 5 km thick layer in the lower troposphere (characteristic height of the PBL). The number of particles in the size distribution was scaled to produce column AOD of 0.5 at 0.5 μm. The refractive index of dust was taken from the WRF-Chem model. The characteristic values of the imaginary part is 10^{-3} in shortwave and 0.65 at 10 μm. The shortwave and longwave spectra were discretized with 10 cm^{-1} step. Figure S1 shows the corresponding spectral optical properties of dust, while Figure S2 shows the CDFs, i.e. the relative contribution of the dust particles as the radius increases.

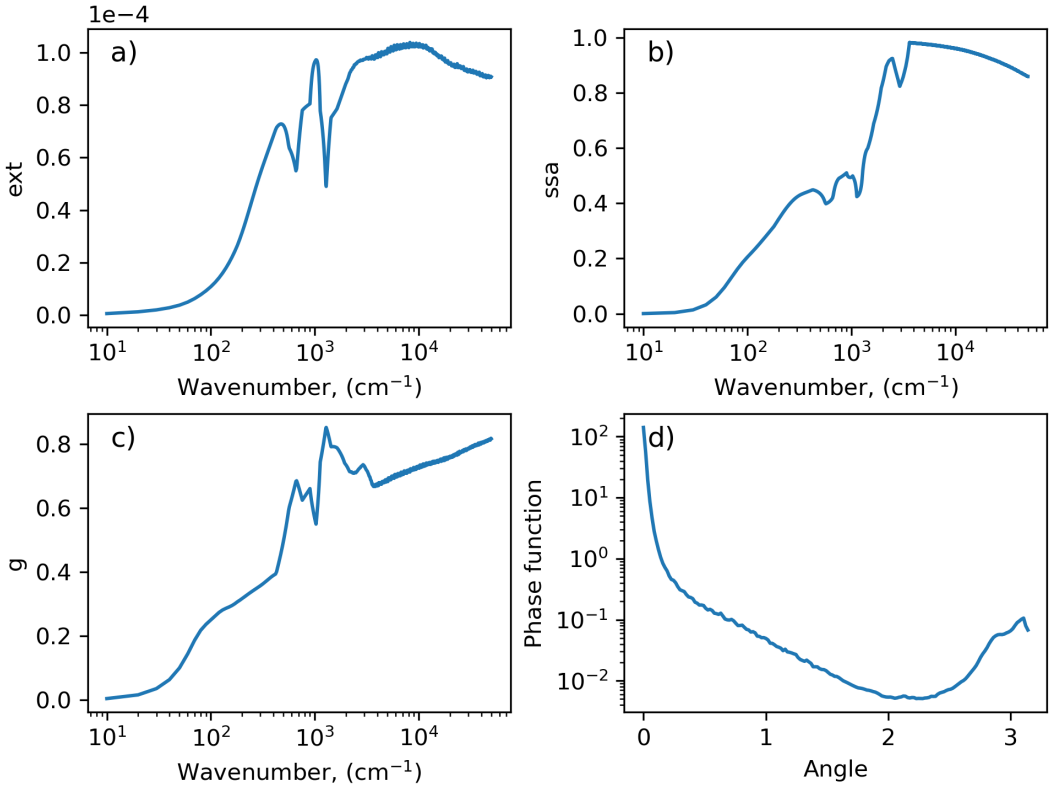

Figure S1: a) Spectral extinction, b) single-scattering albedo, c) asymmetry parameter, and d) phase function for the dust PSD observed after the Haboob dust storm in Saudi Arabia on 9 April 2009. The corresponding dust size distribution is shown in the main text (Figure 11, left column). The number of particles was normalized to produce column AOD of 0.5 at 0.5 μm.

Table S1: Statistical scores (R, RMSE, and Bias) of DD for particles with r < 5 μm simulated within WRF-Chem, MERRA2, and CAMS compared to observations for 2016.

	R	RMSE	Bias
WRF-Chem (Ukhov et al., 2020)	0.70	0.94	0.31
WRF-Chem (This Study)	0.64	1.04	-0.29
MERRA-2	0.41	1.11	-0.24
CAMS	0.36	1.14	0.29

References

Mok, J., Krotkov, N. A., Arola, A., Torres, O., Jethva, H., Andrade, M., ... others (2016). Impacts of brown carbon from biomass burning on surface uv and ozone photochemistry in the amazon basin. *Scientific reports*, *6*(1), 1–9.

Osipov, S., Stenchikov, G., Brindley, H., & Banks, J. (2015). Diurnal cycle of the dust instantaneous direct radiative forcing over the arabian peninsula. *Atmospheric Chemistry and Physics*, *15*(16), 9537–9553.

Osipov, S., Stenchikov, G., Tsigaridis, K., LeGrande, A. N., & Bauer, S. E. (2020). The role of the so radiative effect in sustaining the volcanic winter and soothing the toba impact on climate. *Journal of Geophysical Research: Atmospheres*, *125*(2), e2019JD031726.

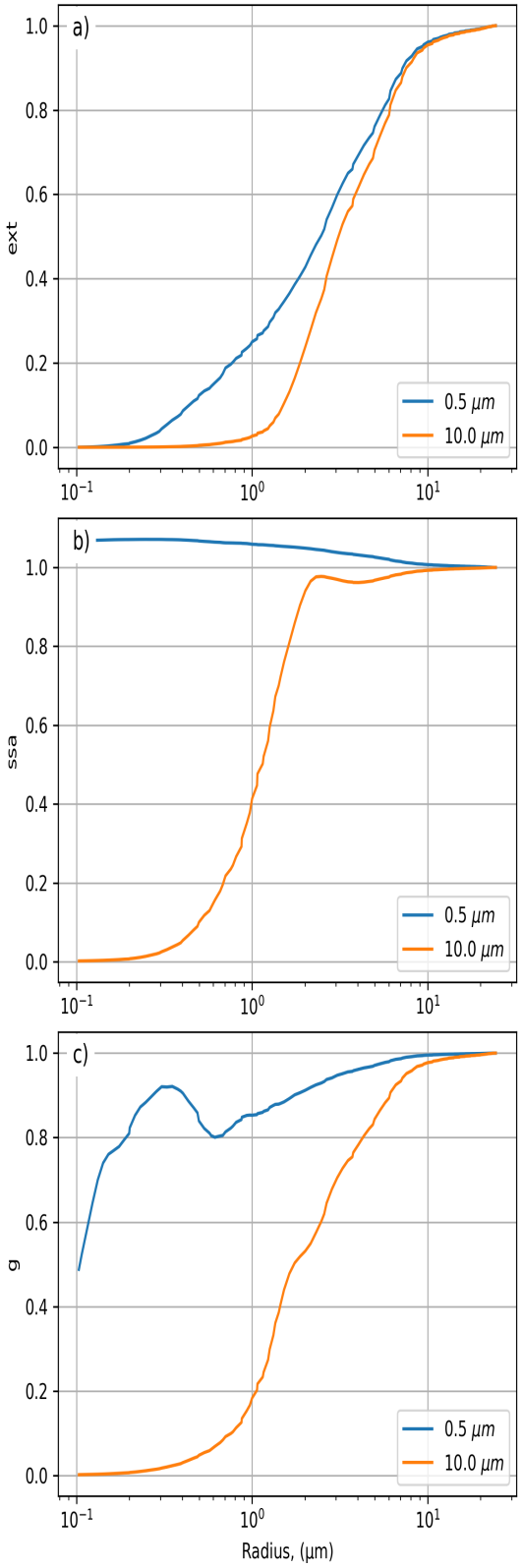

Figure S2: Relative contribution (CDFs) of the dust particles up to radius r to the SW and LW dust optical properties: a) extinction, b) single-scattering albedo, and c) asymmetry parameter shown in Figure S1.

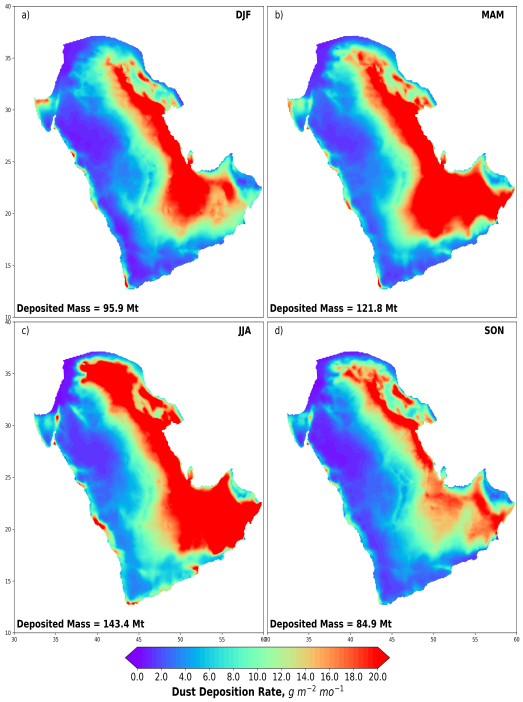

Figure S3: Seasonal mean dust deposition rate $g\ m^{-2}\ mo^{-1}$ in the Arabian Peninsula calculated in WRF-Chem with the DD constraints for 2016: a) DJF, b) MAM, c) JJA, and d) SON. The spatially integrated mass of deposited dust is shown in each panel at the bottom.

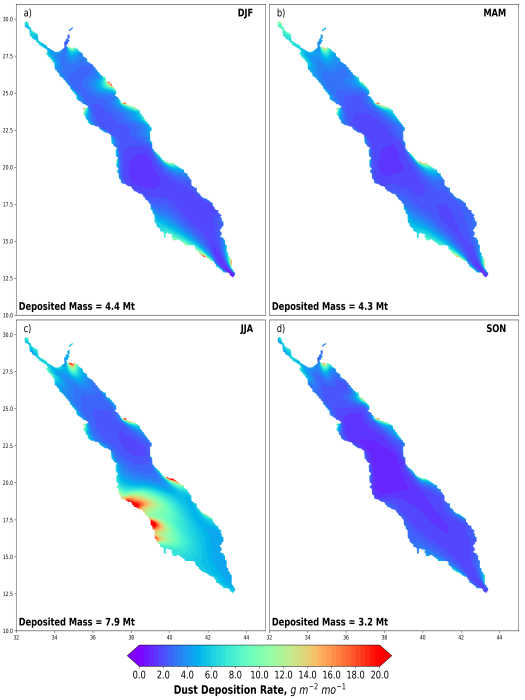

Figure S4: Seasonal mean dust deposition rate $g\ m^{-2}\ mo^{-1}$ in the Red Sea calculated in WRF-Chem with the DD constraints for 2016: a) DJF, b) MAM, c) JJA, and d) SON. The spatially integrated mass of deposited dust is shown in each panel at the bottom.

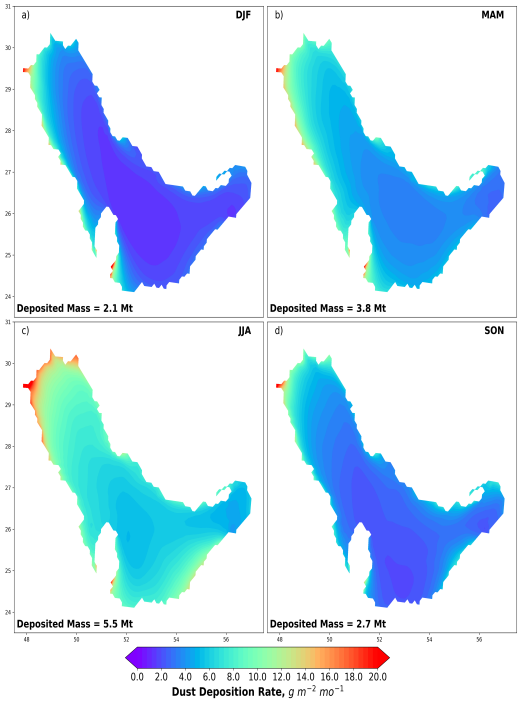

Figure S5: Seasonal mean dust deposition rate $g\ m^{-2}\ mo^{-1}$ in the Arabian Gulf calculated in WRF-Chem with the DD constraints for 2016: a) DJF, b) MAM, c) JJA, and d) SON. The spatially integrated mass of deposited dust is shown in each panel at the bottom.